Energy self-localization and gap local pulses in a two-dimensional nonlinear lattice

J. Pouget
Laboratoire de Modélisation en Mécanique, Université Pierre et Marie Curie, 4, Place Jussieu, 75252 Paris CÉDEX 05, France

M. Remoissenet and J. M. Tamga
Physique Non Linéaire: Ondes et Structures Cohérentes, Faculté des Sciences, 6 blvd Gabriel 21000 Dijon, France
(Received 21 April 1992; revised manuscript received 16 February 1993)

We study the formation of localized states, mediated by modulational instability, on a two-dimensional lattice with nonlinear coupling between nearest particles and a periodic nonlinear substrate potential. Such a discrete system can model molecules adsorbed on a substrate crystal surface, for example. The basic equations of the motion governing the dynamics of the lattice are derived from the model Hamiltonian. In the low-amplitude approximation and semidiscrete limit these equations can be approximated by a two-dimensional nonlinear Schrödinger equation. The modulational instability conditions are calculated; they inform us about the selection mechanism of the wave vectors and growth rate of the instabilities taking place both in the longitudinal and transverse directions. The dynamics of the lattice is then investigated by means of numerical simulations; due to modulational instability an initial steady state that consists of a plane wave with low amplitude modulated by very weak noise, evolves into an oscillating localized state, inhomogeneously distributed on the lattice. These nonlinear localized modes, which move slowly, present the remarkable properties of gap modes. Their amplitude is large and they pulsate at a low frequency that lies inside the lower linear gap of the lattice.

I. INTRODUCTION

Formation and dynamics of localized states in nonlinear systems is of great interest in various branches of physics.[1] Particular interest has been devoted, recently, to the dynamics of structures on two-dimensional systems.[2-3] These structures (dislocations, domains walls, vortices, etc.) play an important role in the material properties and they become crucial in nonlinear physics involved in the problem of adsorbates deposited on crystal surfaces,[4] in superlattices of ultrathin layers, or in large-area Josephson junctions,[5] for instance. Most of the recent literature has focused on dissipative structures in open systems. Nevertheless, it is also important to examine conservative systems which are often concerned the physics of materials at the microscopic level. In this context, it is interesting to consider the response of a system to an initial disturbance and possible energy localization, that is, to study how an initial homogeneous and weak energy distribution may induce the formation of localized states with large amplitude.

In this paper we focus on the formation of localized states mediated by modulational instability in a two-dimensional lattice. The paper is organized as follows. In Sec. II, we introduce our model which is a two-dimensional nondissipative Frenkel-Kontorova model with additional nonlinear interactions. In the low-amplitude and semidiscrete limit, the basic equations governing the dynamics of the lattice are reduced to a two-dimensional nonlinear Schrödinger equation. Then, in Sec. III, the modulational instability conditions of this equation are calculated. Section IV deals with numerical simulations, we investigate the role played by modulational instability on the evolution into localized states of an initial plane wave, with low amplitude, propagating on the lattice. Section V is denoted to a summary and concluding remarks.

II. THE MODEL

A. The basic discrete model

The basic model is made of a two-dimensional (2D) lattice equipped, at each node, with a *rotator* or *rigid rotating molecule.* Namely, each molecule can rotate in the lattice plane. At site (m,n) the angle of rotation is $\Phi_{m,n}$ (see Fig. 1). Each molecule interacts *nonlinearly* with its first-nearest neighbors and with a *periodic substrate potential.* Under these conditions the Hamiltonian is

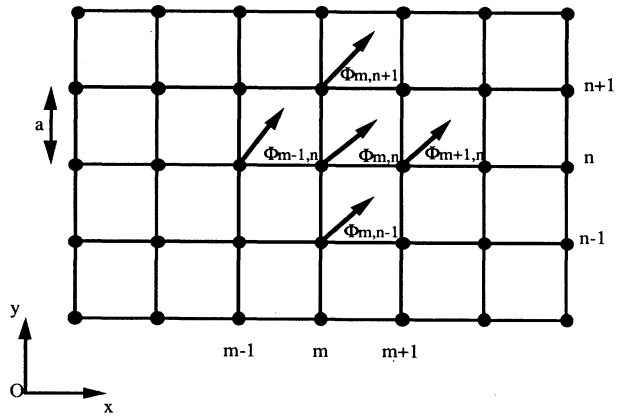

FIG. 1. The two-dimensional lattice model equipped, at each node, with a rigid rotating molecule; a denotes the lattice spacing and $\Phi_{m,n}$ represents the orientation of molecule at site (m,n).

$$H=J\sum_{m,n}\left[\frac{1}{2}\dot{\Phi}^2_{m,n}+\frac{G_L}{2J}(\Phi_{m+1,n}-\Phi_{m,n})^2+\frac{G_T}{2J}(\Phi_{m,n+1}-\Phi_{m,n})^2+\frac{B_L}{4J}(\Phi_{m+1,n}-\Phi_{m,n})^4 + \frac{B_T}{4J}(\Phi_{m,n+1}-\Phi_{m,n})^4+\omega_0^2(1-\cos\Phi_{m,n})\right] . \quad (1)$$

Here, J is the inertia of the molecules, G_L and G_T are the linear coupling coefficients in the longitudinal and transverse directions, while the parameters B_L and B_T are the nonlinear coupling coefficients in the longitudinal and transverse directions, respectively. The last term in relation (1) is due to the substrate potential where ω_0^2 is the strength of the potential barrier and ω_0 can be interpreted as the frequency of small oscillations in the bottom of potential wells. Note in passing that the nonlinear interaction terms can be thought of as the first terms in the expansion of cosine of angles differences. The equation of motion of the molecule at site (m,n) derived from Hamiltonian (1) is

$$\ddot{\Phi}_{m,n}=\frac{G_L}{J}(\Phi_{m+1,n}+\Phi_{m-1,n}-2\Phi_{m,n})+\frac{G_T}{J}(\Phi_{m,n+1}+\Phi_{m,n-1}-2\Phi_{m,n}) + \frac{B_L}{J}[(\Phi_{m+1,n}-\Phi_{m,n})^3-(\Phi_{m,n}-\Phi_{m-1,n})^3] + \frac{B_T}{J}[(\Phi_{m,n+1}-\Phi_{m,n})^3-(\Phi_{m,n}-\Phi_{m,n-1})^3]-\omega_0^2\sin\Phi_{m,n} . \quad (2)$$

Note that if the nonlinear couplings are removed ($B_L=0$ and $B_T=0$), Eq. (2) reduces to the 2D Frenkel-Kontorova or 2D discrete sine-Gordon model.[6] As we shall see in the following, this nonlinear coupling will play an important role in the instability conditions.

B. Nonlinear dispersion relation

In this section we derive the nonlinear dispersion relation corresponding to (2): this relation represents the key equation which, in the weak-amplitude limit, allows us to reduce Eq. (2) to 2D *nonlinear Schrödinger equation.* To calculate the nonlinear dispersion relation, we assume *plane-wave solutions* with slowly varying envelope of the form

$$\Phi_{m,n}(t)=\epsilon\psi_{m,n}\exp[i(\omega t-k_L ma-k_T na)]+\text{c.c.} \quad (3)$$

Here c.c. denotes the complex conjugate, k_L and k_T are the components of the wave vector $\mathbf{k}=(k_L,k_T)$, ω is the circular frequency of the carrier wave which varies rapidly, and $\epsilon\ll 1$. The small-amplitude limit is considered, this allows us to expand the sine function with respect to $\Phi_{m,n}$ up to the third order. On inserting (3) into (2) and neglecting the third-order harmonic terms we obtain the *nonlinear dispersion relation*

$$\omega^2=\omega_0^2+4\frac{C_{0L}^2}{a^2}\sin^2\left[\frac{k_L a}{2}\right]+4\frac{C_{0T}^2}{a^2}\sin^2\left[\frac{k_T a}{2}\right] +\epsilon^2\left[\frac{48B_L}{J}\sin^4\left[\frac{k_L a}{2}\right] +\frac{48B_T}{J}\sin^4\left[\frac{k_T a}{2}\right]-\frac{1}{2}\omega_0^2\right]|\psi|^2 , \quad (4)$$

where $C_{0L}^2=G_L a^2/J$ and $C_{0T}^2=G_T a^2/J$. The first three terms in the right-hand side of Eq. (4) represent the linear contribution to the dispersion relation whereas the last term corresponds to the nonlinear contribution. In the above calculations we have used the continuum approximation and the slow envelope was considered as constant in comparison to the rapid carrier oscillations.

C. Derivation of the 2D nonlinear Schrödinger equation

To reduce Eq. (2) to a 2D nonlinear Schrödinger (2D-NLS) equation we can use the multiple scale perturbative technique or consider the nonlinear dispersion relation (4). We have verified that both methods give the same result. Here, for sake of clarity we present the second method. Namely, if we consider slow modulation in space and time of a carrier wave with given wave numbers k_{Lc} and k_{Tc} and expand the dispersion relation (4) around the carrier parameters $(k_{Lc},k_{Tc};\ |\psi|^2=0)$, we arrive at

$$\omega-\omega_c=(k_L-k_{Lc})\left[\frac{\partial\omega}{\partial k_L}\right]_c+(k_T-k_{Tc})\left[\frac{\partial\omega}{\partial k_T}\right]_c+\tfrac{1}{2}(k_L-k_{Lc})^2\left[\frac{\partial^2\omega}{\partial k_L^2}\right]_c + \tfrac{1}{2}(k_T-k_{Tc})^2\left[\frac{\partial^2\omega}{\partial k_T^2}\right]_c+(k_L-k_{Lc})(k_T-k_{Tc})\left[\frac{\partial^2\omega}{\partial k_L\partial k_T}\right]_c+\left[\frac{\partial\omega}{\partial|\psi|^2}\right]_c|\psi|^2 , \quad (5)$$

where the subscript c denotes evaluation at ω_c, $k_L=k_{Lc}$, $k_T=k_{Tc}$, $|\psi|^2=0$. The frequency ω_c is the carrier frequency and it is provided by the linear part of the dispersion relation (4). Let the operators $k_L-k_{Lc}=-i\epsilon\partial/\partial X$, $k_T-k_{Tc}=-i\epsilon\partial/\partial Y$, and $\omega-\omega_c=i\epsilon\partial/\partial t_1$. Here, $X=\epsilon x$, $Y=\epsilon y$, $t_1=\epsilon t$ (with $\epsilon\ll 1$) represent the slow variables appropriate to the slow envelope variation. On applying these operators to the amplitude function $\psi(X,Y,T)$, we obtain the following equation:

$$i\epsilon(\psi_{t_1}+V_{gL}\psi_X+V_{gT}\psi_Y)+\epsilon^2P_1\psi_{XX}+\epsilon^2P_2\psi_{YY}+\epsilon^2P_3\psi_{XY}+\epsilon^2Q|\psi|^2\psi=0\ , \quad (6)$$

where

$$P_1=\frac{1}{2}\left[\frac{\partial^2\omega}{\partial k_L^2}\right]_c,\quad P_2=\frac{1}{2}\left[\frac{\partial^2\omega}{\partial k_T^2}\right]_c,$$

$$P_3=\left[\frac{\partial^2\omega}{\partial k_L\partial k_T}\right]_c,\quad Q=-\left[\frac{\partial\omega}{\partial|\psi|^2}\right]_c,$$

$$V_{gL}=\left[\frac{\partial\omega}{\partial k_L}\right]_c,\quad V_{gT}=\left[\frac{\partial\omega}{\partial k_T}\right]_c.$$

These coefficients, which represent the dispersion, the nonlinearity, and the group velocities, are given in Appendix A. Without loss of generality, attention can be restricted to the case of carrier wave propagating in the x direction, i.e., $k_{Lc}=k_c$ and $k_{Tc}=0$. Under this condition P_3 and V_{gT} become zero (see Appendix A) and Eq. (6) can be rewritten as

$$i\epsilon(\psi_{t_1}+V_{gL}\psi_X)+\epsilon^2P_1\psi_{XX}+\epsilon^2P_2\psi_{YY}+\epsilon^2Q|\psi|^2\psi=0\ . \quad (7)$$

Considering a frame moving with group velocity V_{gL} and using the transformation $\xi=X-V_{gL}t_1$, $\eta=Y$, $\tau=\epsilon t_1$, next (V_{gL} being the group velocity in the longitudinal direction) we transform Eq. (7) into the standard 2D nonlinear Schrödinger equation:

$$i\psi_\tau+P_1\psi_{\xi\xi}+P_2\psi_{\eta\eta}+Q|\psi|^2\psi=0\ , \quad (8a)$$

where

$$P_1=[C_{0L}^2\omega_c^2a^2\cos(k_ca)-C_{0L}^4\sin^2(k_ca)]/2a^2\omega_c^3\ , \quad (8b)$$

$$P_2=C_{0T}^2/2\omega_c\ , \quad (8c)$$

$$Q=\left[\frac{1}{2}\omega_0^2-48\frac{B_L}{J}\sin^4\left[\frac{k_ca}{2}\right]\right]\Big/2\omega_c\ . \quad (8d)$$

At this point, it is important to note that for a given k_c the sign of Q can be modified by changing the value of B_L which represents nonlinear coupling. Equation (8a) has been extensively studied especially in plasma physics, hydrodynamics, and optics.[7] We now restrict our study to the isotropic case, i.e., $G_L=G_T=G$ ($C_{0L}=C_{0T}=C_0$) and $B_L=B_T=B$. Proceeding as Yuen and Lake[8] for their study of hydrodynamic waves, it is convenient to reduce Eq. (8a) to a 1D equation, that is, consider plane modulation at an angle α from the direction of propagation of carrier wave. Namely, we introduce the oblique coordinate

$$S=\xi\cos\alpha+\eta\sin\alpha\ .$$

Equation (8a) is then transformed into the 1D nonlinear Schrödinger equation

$$i\psi_\tau+P\psi_{SS}+Q|\psi|^2\psi=0\ , \quad (9)$$

where the coefficient P is given by

$$P=\frac{-4C_0^4\cos^2\alpha\sin^4(k_ca/2)+(4C_0^4\sin^2\alpha-2\omega_0^2a^2C_0^2\cos^2\alpha)\sin^2(k_ca/2)+C_0^2\omega_0^2a^2}{2\omega_c^3a^2}\ . \quad (10)$$

Equation (9) describes the evolution of the envelope ψ in the S direction of a carrier wave propagating in the x direction.

III. MODULATIONAL INSTABILITY

Equation (9) has a plane-wave solution of constant amplitude of the form

$$\psi=\psi_0\exp(i\Omega\tau)\ , \quad (11)$$

where ψ_0 and Ω are constants satisfying

$$\Omega=Q\psi_0^2\ .$$

We now investigate the *Benjamin-Feir* or *modulation instability*[9] of the plane wave given by (11) to a perturbation of the form

$$\psi=[\psi_0+\epsilon A(S,\tau)]\exp\{i[Q\psi_0^2\tau+\epsilon\varphi(S,\tau)]\}\ , \quad (12)$$

where $A(S,\tau)$ and $\varphi(S,\tau)$ are real functions and ϵ is a small parameter. Inserting (11) into (9) we obtain at $O(\epsilon)$

$$A_\tau+P\psi_0\varphi_{SS}=0\ , \quad (13a)$$

$$\varphi_\tau=\frac{P}{\psi_0}A_{SS}+2Q\psi_0A\ , \quad (13b)$$

we seek a solution to (13) in the form

$$A(S,\tau)=A_0\exp[i(\nu\tau-qS)]+\text{c.c.}\ , \quad (14a)$$

$$\varphi(S,\tau)=\varphi_0\exp[i(\nu\tau-qS)]+\text{c.c.}\ , \quad (14b)$$

where A_0,φ_0 are real constants, q is a real wave number, and ν may be complex. Here, c.c. is used to denote the complex conjugate. Substituting (14) into (13) leads to the following linear system:

$$i\nu A_0 - Pq^2\psi_0\varphi_0 = 0 \ , \tag{15a}$$

$$\left[\frac{P}{\psi_0}q^2 - 2Q\psi_0\right]A_0 + i\nu\varphi_0 = 0 \ , \tag{15b}$$

the condition for a nontrivial solution gives the dispersion relative

$$\nu^2 = P^2q^2\left[q^2 - 2\psi_0^2\frac{Q}{P}\right] . \tag{16}$$

If the right-hand side is negative then the angular frequency ν will be complex and the perturbation will grow. In this case, the *region of instability* is given by

$$0 < q < q_l \ . \tag{17}$$

The explicit expression for $q_l = \psi_0\sqrt{2Q/P}$ is given in Appendix B. Thus, a perturbation with a wave vector $\mathbf{q} = (q_L, q_T)$ satisfying

$$0 < q_L < q_l \cos\alpha, \quad 0 < q_T < q_l \sin\alpha$$

can trigger instability in the lattice. Here q_L and q_T are the wave numbers of the perturbation in the longitudinal and transverse directions. α is an angle defined by $\alpha = \tan^{-1}(q_L/q_T)$. The maximum instability occurs at

$$q_{L\max} = (q_l/\sqrt{2})\cos\alpha, \quad q_{T\max} = (q_l/\sqrt{2})\sin\alpha$$

with a maximum growth rate given by $\sigma_{\max} = |\nu| = Q\psi_0^2$. The modulational instability criterion depends on the sign of PQ which depends itself on the carrier wave number and on the modulation propagation direction for $\alpha = 0$ the instability is longitudinal, for $\alpha = \pi/2$ the instability is transverse. In the first Brillouin zone three cases are possible (see Appendix C): (i) for $0 < k_c < k_{c2}$, $PQ > 0$ for all α; (ii) for $k_{c2} < k_c < k_{c1}$, PQ is always negative; (iii) if $k_{c1} < k_c < \pi/a$, then we have $PQ > 0$ for $\alpha < \alpha_c$ and $PQ < 0$ for $\alpha > \alpha_c$. In this last case, like for hydrodynamic waves,[8] there is a limiting angle which can be calculated from model parameters. However, in the following the influence of this limiting angle will not be examined. We will restrict ourselves to case (i). For this case, we have plotted in Fig. 2 the growth rate $\sigma = |\nu|$ versus q for the set of parameters $\omega_0 = 0.3$, $C_0 = 1$, $k_c = 0.415$, $\alpha = \pi/2$ for two different values of B: $B = 0$, $B = 0.1$.

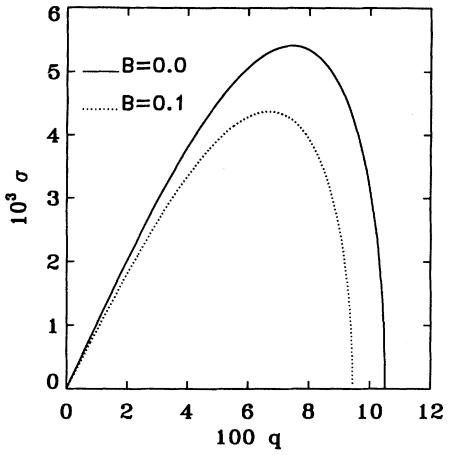

FIG. 2. Growth rate $\sigma = |\nu|$ vs q for the set of parameters $\omega = 0.3$, $C_0 = 1$, $k_c = 0.415$, $\alpha = \pi/2$ for two different values of B: the solid line is for $B = 0$ and the dashed line is for $B = 0.1$

IV. NUMERICAL SIMULATIONS

The previous theoretical results tell us that in the semidiscrete and low-amplitude limit the dynamics of the lattice can be approximatively described by a 2D-NLS equation. This equation allows us to predict instabilities but not their evolution as time increases. In this section we want to clarify the role played by these modulational instabilities on the response of the lattice to an initial homogeneous disturbance with low amplitude. Furthermore, we attempt to elucidate the exact nature of the nonlinear structures which should appear in the long-time evolution of the lattice and cannot be predicted from the 2D-NLS model. At this end we use numerical simulations which are directly performed on the original microscopic equations [see Eq. (2)] which govern the dynamics of 2D lattice. Specifically, we consider a lattice plane made of 106×82 points along with periodic boundary conditions on left and right sides and on lower and upper boundaries, as well. The initial conditions are provided by a harmonic wave carrier traveling in the x direction and homogeneous in the transverse direction. These initial conditions are chosen to be

$$\Phi(m,n) = 2A\sin[k_c(m - m_0)] \ , \tag{18a}$$

$$\dot{\Phi}(m,n) = -2\omega A\cos[k_c(m - m_0)] \ , \tag{18b}$$

where A is the amplitude, m_0 is an initial position, k_c is the wave number of the carrier, and ω the corresponding circular frequency which satisfies the dispersion relation (3) where $k_T = 0$. This dispersion relation implies a nonzero phase velocity because a forbidden band exists for $0 < \omega < \omega_0$ as given by Eq. (4) in the linear limit. We have seven periods within the longitudinal length of the lattice plane which leads to $k_c \simeq 0.415$ the corresponding circular frequency is $\omega = 0.509$. In order that our initial condition (plane wave) satisfies the nonlinear Schrödinger approximation, we have take $2A = 0.7$. It means that the maximum of the initial collective angular motion of the rotations is equal to $\pi/6$. Note that this value is small compared to the amplitude (slightly larger than π) necessary to overcome the potential barrier. In order to trigger the instability, small ($\simeq 10^{-3}$) random or coherent perturbations are superposed to the initial velocity $\dot{\Phi}$ and removed afterwards. We have first checked that for $\alpha = \pi/2$ a small modulation gives rise to transverse instability. Otherwise in the longitudinal case, that is for $\alpha = 0$, we recover the classical modulational instability for a 1D system: the initial sinusoidal wave breaks into a train of envelope solitons.

We consider, here, two sets of numerical simulations. The first set of simulations is carried out for the discrete sine-Gordon system, that is, with zero nonlinear coupling ($B = 0$). In dimensionless units, the strength of the substate potential is $\omega_0^2 = 0.09$ and we have chosen $C_0 = 1$, $a = 1$. The square of the quantity $C_0/\omega_0 = d$ represents

the ratio of linear coupling energy to the strength of the potential barrier. Here, in physical units we have $d=3.3a$. This choice corresponds to a real physical system where the estimated values of the relevant parameters are $a=2.5$ Å, $C_0=3\times10^3$ m s^{-1}, $\omega_0=3.6\times10^{12}$ rad s^{-1}, which corresponds to a wave number of about 20 cm^{-1} in a spectroscopic experiment. Under these conditions we find $\omega=6.1\times10^{12}$ rad s^{-1} and $k_c=16\times10^6$ cm^{-1} for the initial plane wave. The results are collected together in Fig. 3 where we have the contour line plots for $\mathrm{sgn}(\Phi)\Phi^2$. Figure 3(a) shows the structures at initial time $T=0$. The corresponding power spectrum is drawn in Fig. 4(a) where one peak at the carrier wave number is present. Then, as predicted by the NLS model, the instability occurs and after a lapse of time $T=1280$, the small initial perturbation gives rise to stretched localized structures along the transverse direction. At time $T=3500$, we observe very clearly some localized structures which are ellipse-shaped as shown in Fig. 3(c). They look like the ring solitons or pulsons observed numerically in the 2D sine-Gordon system with different boundary conditions.[10] When time further increases, we observe [see Fig. 3(d)] that these localized structures still persist and look like stable. No recurrence to the initial state of these structures, in the Fermi-Pasta-Ulam sense, was observed for these set of simulations. The characteristic extends of these structures are about 10 lattice spacings in the x direction and 21 lattice cells in the y direction. We attribute this anisotropy to the discreteness effects which could be important in the x direction while the continuum limit seems to be acceptable in the transverse direction. The corresponding power spectrum is given in Fig. 4(b) where additional peaks at $q_y\neq0$ are present, this proves that transverse modulation components have grown. In Fig. 5, we have represented the finite differences gradient of the rotation $\Phi_{m,n}$ in the x and y directions. The resulting structures present some similarities with vortexlike structures. In order to obtain more details about the dynamics of a particular structure we have plotted the profile, in the x direction, of the struc-

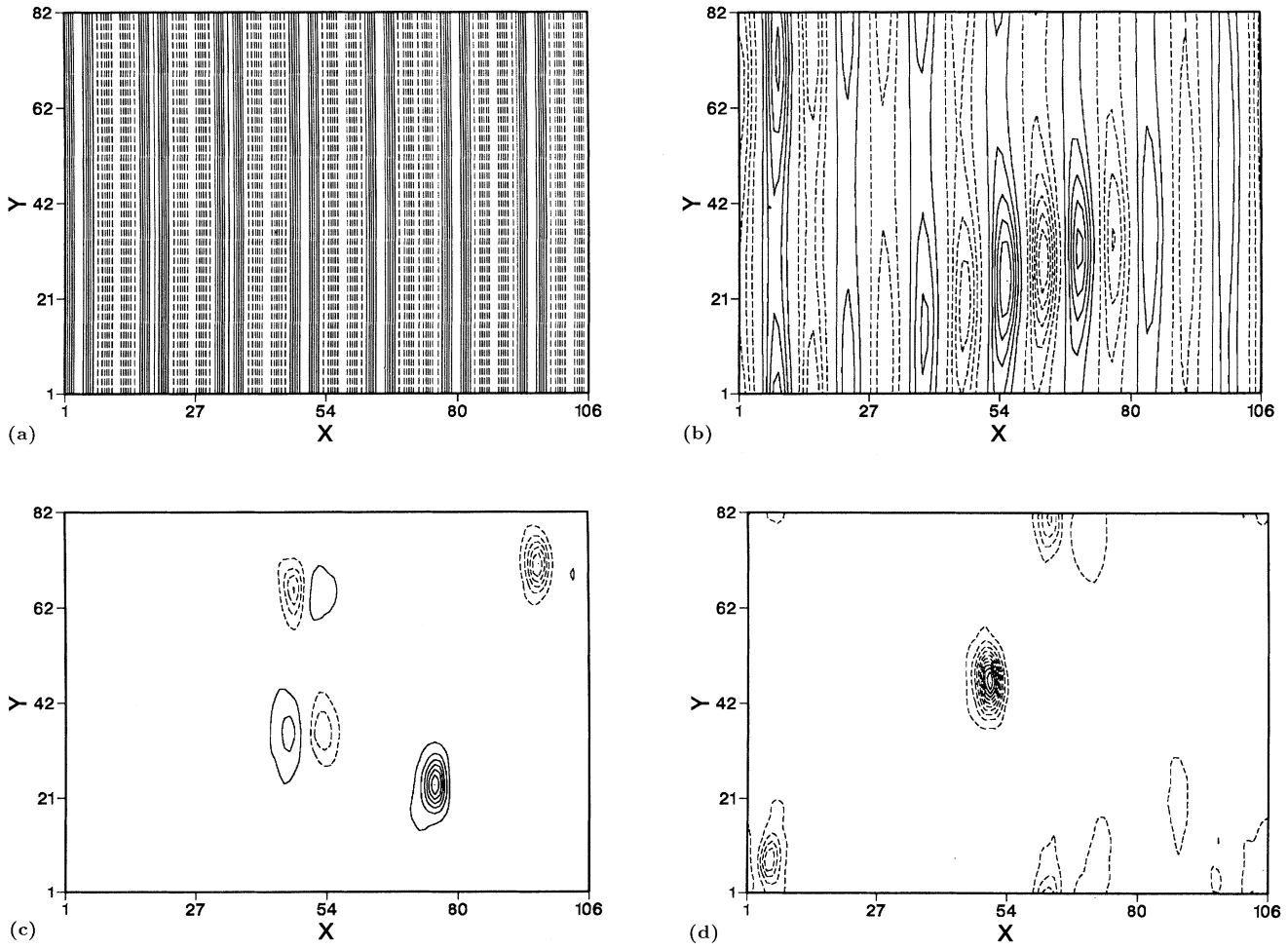

FIG. 3. Contour line plots corresponding to Φ^2 at various times for the pure sine-Gordon system (the solid line is for $\Phi>0$, the dashed line is for $\Phi<0$). (a) Initial structure: periodic carrier in the x direction, (b) the birth of localized structures at time $T=1280$, (c) moving pulsons at time $T=3500$, and (d) the evolution of the pulson later on, at time $T=4240$.

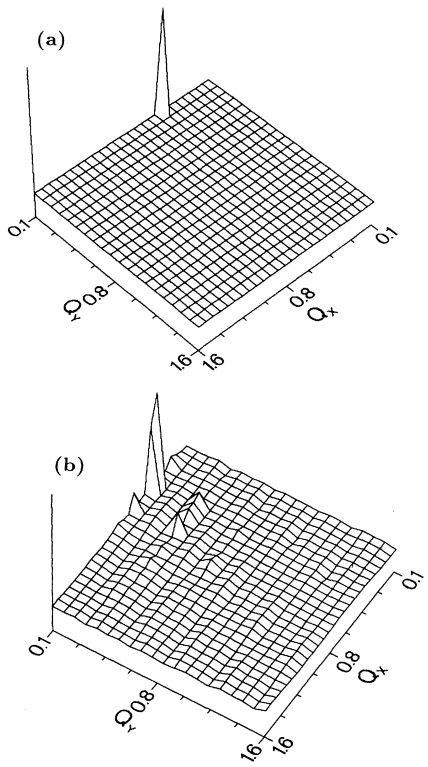

FIG. 4. Power spectrum of the rotation angle Φ, (a) at initial time, only the peak at the carrier wavelength is present, and (b) at time $T=4240$, the spectrum exhibits additional peaks at nonzero transverse wave numbers.

ture located in the middle of the lattice between times $T=4200$ and 4245, the results are shown in Figs. 6(a) and 6(b). It is now clear that the structure is moving in the x direction while oscillating like a breather or a pulson. From these results we can estimate the traveling velocity of the pulson $V_{\text{trav}} \simeq 0.55$ and its circular frequency: $\Omega \simeq 0.2$. It is very interesting to note that this frequency is smaller than the cutoff frequency $\omega_0=0.3$: it lies in the lower linear gap of the lattice. Thus, in an experiment the oscillations of the pulsons could be detected for wave numbers of about $(0.2/0.3)\times 20\ \text{cm}^{-1} \simeq 13\ \text{cm}^{-1}$. Finally, we note that the amplitude of the pulsons is large and such that $-4\pi/3 < \Phi < 4\pi/3$, thus the (molecular) rotations overcome collectively the potential barrier, but they do not reach the bottom of the next well. Our simulations also show (not represented here) that the number of pulsons decreases whereas their spatial extension increases with the ratio $d=C_0/\omega_0^2$. We can roughly explain this behavior by considering that the energy localized by modulational instability, allows in some places collective particle motions. Thus, if $d \gg 1$, the particles have an important probability to overcome collectively the potential barrier over large distances giving rise to a small number of extended pulsons. On the contrary, if d decreases, the probability of collective jump decreases with distance, the number of pulsons increases whereas their dimensions are reduced. Nevertheless, this problem must be further carefully investigated.

Next, a second series of simulations is considered, for which the competing nonlinear coupling term is taken into account ($B=0.1$). We use same initial conditions as previously [see Fig. 3(a)]. Typically, we recover the same results as in the case of the discrete sine-Gordon system. The set of Figs. 7(a)–7(c) corresponds to the birth of the

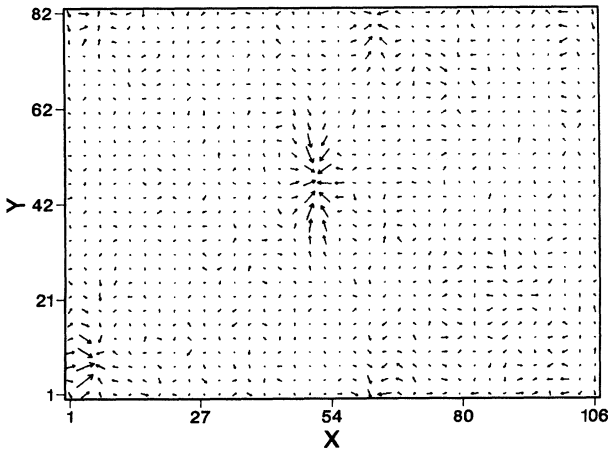

FIG. 5. Patterns corresponding to Fig. 3(d). The arrows depict the rotation gradient.

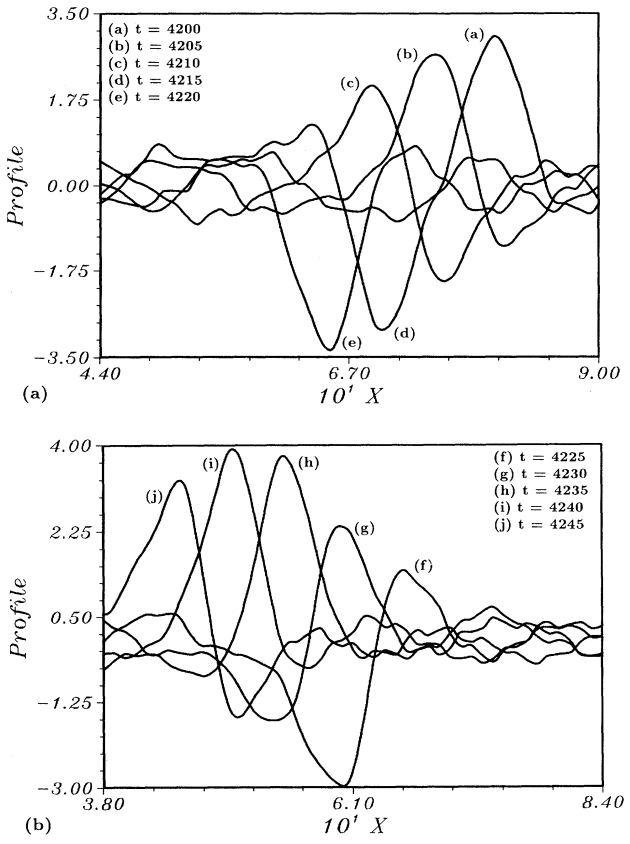

FIG. 6. Evolution of the profile of a typical structure (a) $4200 \le T \le 4220$ and (b) $4225 \le T \le 4245$. The profile shows that the pulson breathes while moving in the x direction.

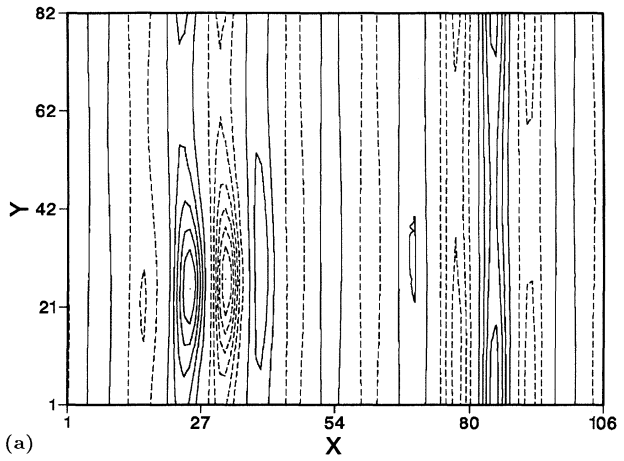

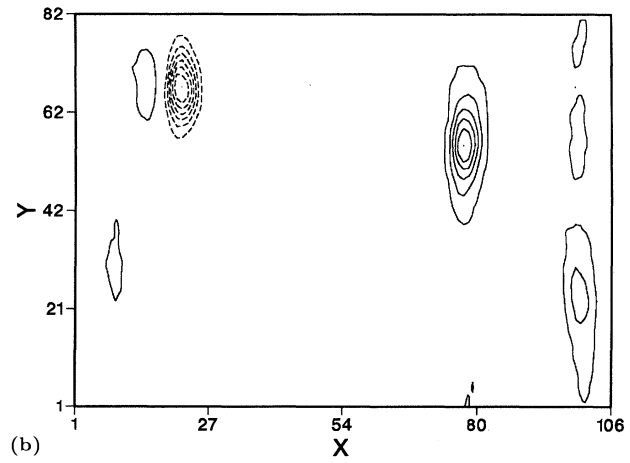

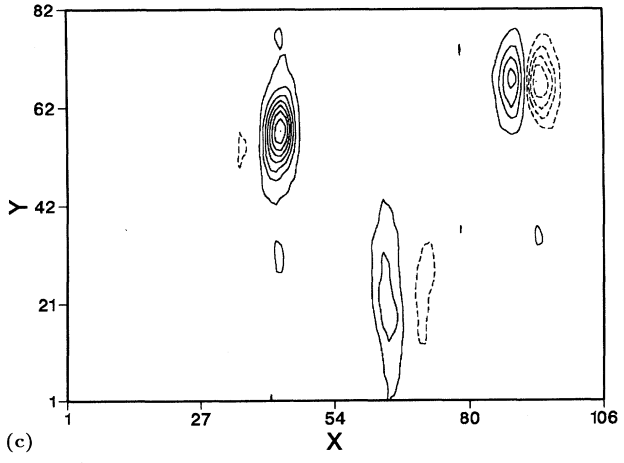

FIG. 7. Lattice dynamics when the nonlinear coupling is included: contour line plots of the rotation amplitude Φ^2. (a) The birth of pulsons at $T=1700$, (c) pulsons at $T=5056.4$, and (d) the pulsons a short time later at $T=5098.8$.

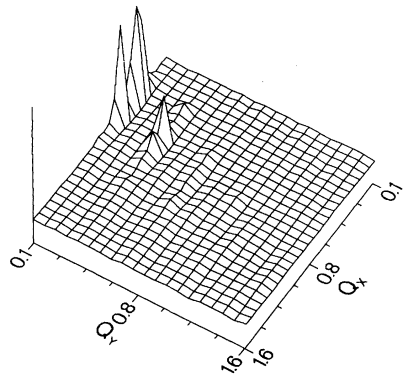

FIG. 8. Spatial power spectrum of the lattice at $T=5098.8$ exhibiting peaks beside the carrier peak.

structures formation, the localized structures, and the dynamics of these nonlinear structures for a long time, respectively. It is worthwhile noting that when the nonlinear coupling exists, the transverse instabilities appear more slowly than in the case of the discrete sine-Gordon system. In fact [Eq. (8d)], we can see that the nonlinear coupling decreases the coefficient Q of the nonlinear Schrödinger equation. Under this condition the growth rate $\sigma=|\nu|$ [see Eq. (16)] is smaller than for the case $B=0$. For example, $\sigma=0.0054$ for $B=0$ whereas $\sigma=0.0044$ for $B=0.1$. The power spectrum corresponding to the structures at time $T=5080$ is depicted in Fig. 8. The structures corresponding to the gradient of Φ are presented in Fig. 9. These patterns are rather similar to those obtained by Ishimo and Miyamoto in their study of the Gross-Pitaevskii equation.[11-12] At length, Figs. 10(a) and 10(b) represent the evolution of the pulson located near the point (80,55) between times $T=5056.4$ and 5103.4. As in the previous case, the pulson is moving in the x direction while oscillating or breathing. The pulson velocity is $V_{\text{trav}}\simeq 0.8$, its circular frequency is $\Omega\simeq 0.15$, once again it lies in the linear gap. We notice that these

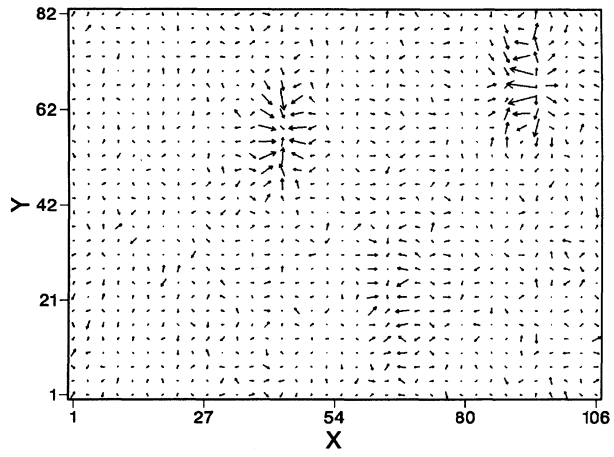

FIG. 9. Patterns corresponding to Fig. 7 at $T=5098.8$. The arrows depict the rotation gradient.

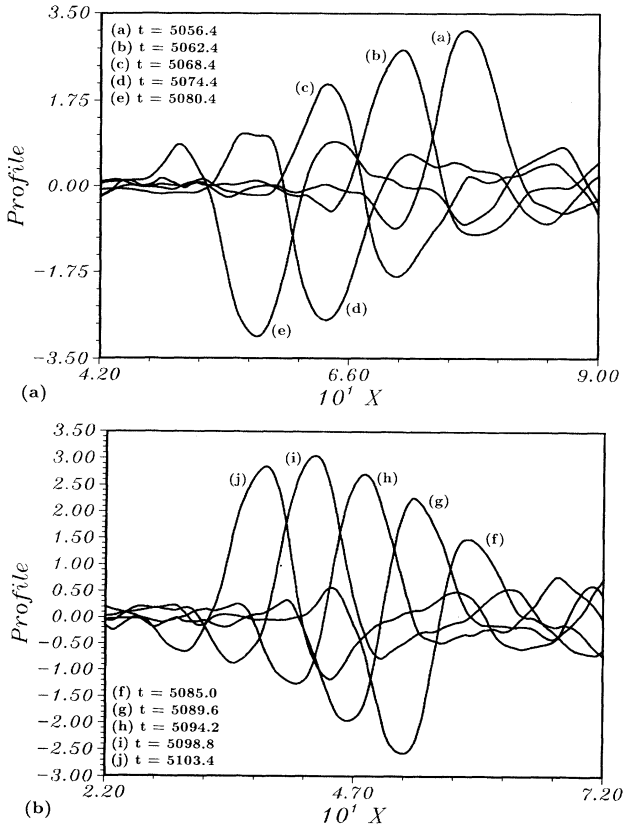

FIG. 10. Dynamics of the profile of the pulson located in the middle of the lattice: (a) $5056.4 \leq T \leq 5080.4$ and (b) $5085.0 \leq T \leq 5103.4$. The pulson oscillates and moves.

important features of the pulsons are different from those obtained for $B=0$. First of all, the velocity is larger but the frequency is lower. Nevertheless, by increasing the nonlinear coupling we can change the sign of the coefficient Q in the nonlinear Schrödinger equation [see Eq. (8d)]. This implies that PQ can become negative and the instabilities disappear as we have checked numerically.

V. SUMMARY AND CONCLUDING REMARKS

We have examined the formation of localized structures, mediated by modulational instability, on a two-dimensional lattice where the first-nearest particles are nonlinearly coupled and experience a periodic nonlinear substrate potential. The basic equations of motion governing the dynamics of the lattice, were derived from the model Hamiltonian. Then, we used the low-amplitude approximation and semidiscrete limit, in which the envelope of the wave is slowly varying whereas the fast oscillations of the quasiharmonic carrier wave are treated exactly, to approximate the equations of motion by a two-dimensional nonlinear Schrödinger equation. Hence, we calculated the modulational instability conditions for a plane-wave propagating along a given direction. Namely, we determined the critical wave-vector range and growth rate of the instabilities of the envelope wave taking place both in longitudinal and transverse directions with respect to the carrier wave.

The response of the lattice to a low-amplitude plane wave modulated by a very weak noise was then investigated by numerical simulations. These simulations were directly performed on the original microscopic equations describing the dynamics of the lattice. In the short time or transient regime our results show that modulational instability appears as we have predicted theoretically. When time further evolves the unstable states break into oscillating localized states or pulsons which move slowly and are inhomogeneously distributed on the lattice. Remarkably, the amplitude of the pulsons is large and their frequency is lower than the cutoff frequency of the linear gap of the lattice. In accordance with our theoretical predictions, our numerical results show that the growth rate of the instability can be reduced and even suppressed if we increase, from zero, the value of the nonlinear coupling term.

In conclusion, our present study shows once more that the complex physics of nonlinear oscillations in extended systems allows the jumping of energy from an initial extended state weakly excited, into local pulses. All our results indicate that the 2D-NLS model is efficient to predict the instabilities of an initial steady state on the lattice. Nevertheless, such a model does not allow one to approach the long-time regime which is characterized by the appearance of remarkable localized objects or pulsons. Moreover, the properties of these pulsons, their number, and their distribution must be further studied both numerically and theoretically. Such problems are currently under investigation.

APPENDIX A

In the general case, the coefficients of the nonlinear Schrödinger equation are given by

$$P_1=\frac{C_{0L}^2\omega_c^2a^2\cos(k_{Lc}a)-C_{0L}^4\sin^2(k_{Lc}a)}{2a^2\omega_c^3}\ , \tag{A1}$$

$$P_2=\frac{C_{0T}^2\omega_c^2a^2\cos(k_{Tc}a)-C_{0T}^4\sin^2(k_{Tc}a)}{2a^2\omega_c^3}\ , \tag{A2}$$

$$P_3=\frac{C_{0L}^2C_{0T}}{a^2\omega_c^2}\sin(k_{Lc}a)\sin(k_{Tc}a)\ , \tag{A3}$$

$$V_{gL}=\frac{C_{0L}^2}{a}\frac{\sin(k_{Lc}a)}{\omega_c}\ , \tag{A4}$$

$$V_{gT}=\frac{C_{0T}^2}{a}\frac{\sin(k_{Tc}a)}{\omega_c}\ , \tag{A5}$$

$$Q=\frac{1}{2\omega_c}\left[\frac{1}{2}\omega_0^2-48\frac{B_L}{J}\sin^4\left[\frac{k_{Lc}a}{2}\right]-48\frac{B_T}{J}\sin^4\left[\frac{k_{Tc}a}{2}\right]\right]\ , \tag{A6}$$

$$\omega_c=\left[\omega_0^2+4\frac{C_{0L}^2}{a^2}\sin^2\left[\frac{k_{Lc}a}{2}\right]+4\frac{C_{0T}^2}{a^2}\sin^2\left[\frac{k_{Tc}a}{2}\right]\right]^{1/2}\ . \tag{A7}$$

We deduce that P_3 and V_{gT} become zero for a carrier wave propagating in the x direction ($k_{Lc}=k_c$ and $k_{Tc}=0$).

APPENDIX B

The explicit expression for q_l (q_l being the limiting wave vector) is the following

$$q_l=\psi_0\left[\frac{2a^2[\omega_0^2+4(C_0^2/a^2)\sin^2(k_ca/2)][(1/2)\omega_0^2-48(B_L/J)\sin^4(k_ca/2)]}{-4C_0^4\cos^2\alpha\sin^4(k_ca/2)+(4C_0^4\sin^2\alpha-2C_0^2\omega_0^2a^2\cos^2\alpha)\sin^2(k_ca/2)+C_0^2\omega_0^2a^2}\right]^{1/2}\ .$$

APPENDIX C

The dispersion coefficient P given by relation (10) can be put into the form

$$P=f(k_c)[g(k_c)-\cos^2\alpha]\ , \tag{C1}$$

where

$$f(k_c)=\frac{4C_0^2\sin^4(k_ca/2)+(4C_0^4+2C_0^2\omega_0^2a^2)\sin^2(k_ca/2)}{2\omega_c^3a^2}\ , \tag{C2}$$

$$g(k_c)=\frac{4C_0^2\sin^2(k_ca/2)+\omega_0^2a^2}{4C_0^2\sin^4(k_ca/2)+(4C_0^2+2\omega_0^2a^2)\sin^2(k_ca/2)}\ . \tag{C3}$$

For $g(k_c)>1$, i.e.,

$$k_c<k_{c1}=(2/a)\sin^{-1}\left[\frac{\omega_0^2a^2+\sqrt{\omega_0^4a^4+4C_0^2\omega_0^2a^2}}{4C_0^2}\right]^{1/2}\ ,$$

P is always positive. Otherwise if $k_c>k_{c1}$, then P is positive for $\alpha>\alpha_c$ and negative for $\alpha<\alpha_c$ where α_c is given by

$$\alpha_c=\cos^{-1}\left[\frac{4C_0^2\sin^2(k_ca/2)+\omega_0^2a^2}{4C_0^2\sin^4(k_ca/2)+(4C_0^2+2\omega_0^2a^2)\sin^2(k_ca/2)}\right]^{1/2}\ . \tag{C4}$$

Let us define the critical wave number k_{c2} for which Q becomes zero. Q is positive for $k_c<k_{c2}$ and negative for $k_c>k_{c2}$. k_{c2} is given by

$$k_{c2}=\frac{2}{a}\sin^{-1}\left[\frac{J\omega_0^2a^4}{96B_L}\right]^{1/4}\ . \tag{C5}$$

In the first Brillouin zone $[0,\pi/a]$, we deduce that if $0<k_c<k_{c2}$, then PQ is positive for all angles. If $k_{c2}<k_c<k_{c1}$, then $PQ<0$ for all α. If $k_{c1}<k_c<\pi/a$ then we have $PQ>0$ for $\alpha<\alpha_c$ and $PQ<0$ for $\alpha>\alpha_c$.

[1] A. V. Gaponov-Grekhop and M. I. Rabinowich, Phys. Today **43**, 30 (1990).

[2] F. Falo, A. R. Bishop, P. S. Lomdahl, and B. Horovitz, Phys. Rev. B **43**, 8081 (1991).

[3] P. Coullet and D. Walgraef, Europhys. Lett. **10**, 525 (1991).

[4] I. F. Lyuksyutov, A. G. Naumovets, and Yu. S. Vedula, in *Soliton in Modern Problem in Condensed Matter Sciences,* edited by S. E. Trullinger, V. E. Zakharov, and V. L. Porovsky (Elsevier Science, New York, 1986), Vol. 17, p. 605.

[5] E. M. Maslov, Physica D **15**, 433 (1985).

[6] J. Pouget, S. Aubry, A. R. Bishop, and P. S. Lomdahl, Phys. Rev. B **39**, 9500 (1989).

[7] V. E. Zakharov, Zh. Eksp. Teor. Fiz. **62**, 1745 (1972) [Sov. Phys. JETP **35**, 908 (1972)].

[8] H. C. Yuen and B. M. Lake, Phys. Fluids **18**, 956 (1975).

[9] T. B. Benjamin and J. E. Feir, J. Fluid Mech. **27**, 417 (1967).

[10] P. L. Christiansen and P. S. Lomdahl, Physica D **2**, 482 (1981).

[11] Y. Ishimori, J. Phys. Soc. Jpn. **55**, 82 (1986).

[12] Y. Ishimori and N. Miyamoto, J. Phys. Soc. Jpn. **55**, 3756 (1986).